

## Oceanic transports through the Solomon Sea: The bend of the New Guinea Coastal Undercurrent

Florent Gasparin,<sup>1</sup> Alexandre Ganachaud,<sup>1,2</sup> Christophe Maes,<sup>1,3</sup> Frédéric Marin,<sup>1,2</sup>  
and Gérard Eldin<sup>1,3</sup>

Received 30 May 2012; revised 29 June 2012; accepted 4 July 2012; published 9 August 2012.

[1] Thermocline waters of the tropical southwest Pacific can be traced back to the center of the South Pacific basin and have a potential influence on equatorial surface conditions and on the characteristics of the El Niño Southern Oscillation on decadal timescales. The Solomon Sea is traversed by this influential flow, and therefore is an optimal place for exploring this oceanic connection to the equator. From a high-resolution hydrographic survey at which we applied an inverse box model, we describe the main pathways at the entrance of the Solomon Sea, and more particularly the extremely sharp bend of the western boundary current around the south-east tip of Papua New Guinea. Of the 30 Sv subtropical waters transported into the Coral Sea from the east, above 1300 m,  $29 \pm 5$  Sv makes its way through the Solomon Sea with a large part transported in a boundary current, at the entrance of the Solomon Sea. Around the south-east tip of Papua New Guinea, the Gulf of Papua Current turns abruptly to the north, in a very sharp bend as it merges into the New Guinea Coastal Undercurrent, on its way, toward the equator. The warm currents transport large amounts of internal energy, with a total of  $1.0 \pm 0.3 \cdot 10^{15}$  W entering the Solomon Sea from the south.

**Citation:** Gasparin, F., A. Ganachaud, C. Maes, F. Marin, and G. Eldin (2012), Oceanic transports through the Solomon Sea: The bend of the New Guinea Coastal Undercurrent, *Geophys. Res. Lett.*, 39, L15608, doi:10.1029/2012GL052575.

### 1. Introduction

[2] In the tropical southwest Pacific, *thermocline* waters, referring to waters in the depth range of 100–300 m, can be traced back to the center of the South Pacific subtropical gyre. These waters follow a peculiar pathway, first flowing westward into the Coral Sea (Figure 1); then arriving at the Australian coast, splitting, with the north branch forming a boundary current that flows equatorward into the Solomon Sea, and ultimately feeding into the Equatorial current system [Grenier *et al.*, 2011]. Because of its potential influence on equatorial surface waters and on the characteristics of the El Niño Southern Oscillation (ENSO) on decadal timescales [Gu and Philander, 1997], this influential

circulation pathway has led to a major research effort, the southwest Pacific Ocean Circulation and Climate Experiment (SPICE) [Ganachaud *et al.*, 2007].

[3] The Solomon Sea is located at the frontier between the South Pacific tropical and equatorial oceanic areas, and it is almost closed to the north by a quasi-continuous archipelago of islands, except for three narrow passages that allow waters to reach the equator (inset of Figure 1). Toward the south, the Solomon Sea is open to the Coral Sea, from Sudest Island to Makira. On the east side of the basin, Indispensable Strait provides an additional passage for tropical waters, between the islands of Makira and Guadalcanal (Figure 1).

[4] The significance of the region to the climate system, and in particular to the conditioning of ENSO, was recognized about 40 years ago [Wyrtki, 1975], leading to the WEPOCS field campaigns [Lindstrom *et al.*, 1987]. But since then, research efforts were mostly focused on equatorial ocean-atmosphere dynamics related to ENSO, and the Solomon Sea has only recently become a new focus of attention with the emergence of the SPICE coordinated efforts [Ganachaud *et al.*, 2007].

[5] Numerical models [Melet *et al.*, 2010] and scattered observations [Andrews and Clegg, 1989; Sokolov and Rintoul, 2000] suggest two thermocline water pathways between the Coral Sea and the equator (inset of Figure 1): one is through the western boundary current which flows northward along Queensland, around the Gulf of Papua and into the Solomon Sea; the second is a direct inflow from the northern Coral Sea to the southern Solomon Sea [Qu and Lindstrom, 2002].

[6] However, the pathways and the transports that are involved at the entrance of the Solomon Sea have not been quantified, leading to a dedicated survey in 2007 (Figure 1). The survey enclosed a box between the northern tip of New Caledonia, Papua New Guinea (PNG) and the Solomon Islands, across the south entrance of the Solomon Sea and the mouth of Indispensable Strait, intersecting the main currents of interest.

### 2. Inverse Box Model

[7] Our data set is based on a hydrographic survey with 47 ocean temperature, salinity, dissolved oxygen profiles and Lowered-Acoustic Doppler Current Profiler (L-ADCP) [Visbeck, 2002], measured from the surface to 2000 m depth (FLUSEC cruise, August 2007 [Maes *et al.*, 2008]). The Ship-mounted ADCP (S-ADCP) also provided continuous recording of the currents in the upper 150 m. An inverse box model is built from three sections that form a closed box (inset of Figure 1) so that we could ensure mass, salt, heat and oxygen conservation within the box and provide error estimates of our diagnostics.

<sup>1</sup>LEGOS, Université de Toulouse, UPS, OMP-PCA, Toulouse, France.

<sup>2</sup>LEGOS, IRD, UMR 5566, Nouméa, New Caledonia.

<sup>3</sup>LEGOS, IRD, UMR 5566, Toulouse, France.

Corresponding author: F. Gasparin, LEGOS, Université de Toulouse, UPS, OMP-PCA, 14, Av. Edouard Belin, F-31400 Toulouse CEDEX, France. (florent.gasparin@legos.obs-mip.fr)

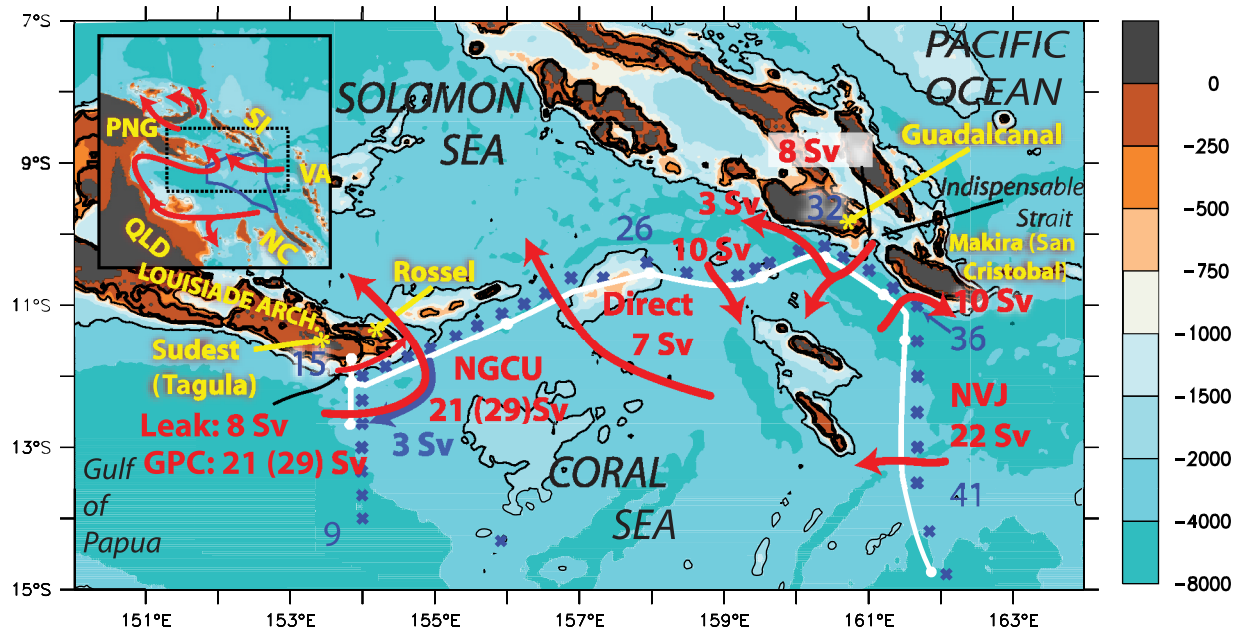


**Figure 1.** Solomon Sea topography, currents and estimated transports. The hydrographic profiles measured during the 2007 hydrographic survey are indicated by the blue crosses; the main water pathways and transports estimated between the surface and  $\sim 1300$  m ( $\sigma_\theta = 27.5$ ) are indicated in red (Sv;  $1\text{ Sv} = 10^6 \text{ m}^3 \text{ s}^{-1}$ ). The transports for the GPC and NGCU, including the *leak*, are given in parenthesis. The white segments indicate the horizontal limits of transport integrals. The 50-m (thick) and 500-m and 2000-m (thin lines) are indicated. Local island names are given in yellow; alternative names used in several nautical charts are given in parenthesis. The inset provides a view of the regional scale current pathways between the Coral Sea and the Equator. Country/Island names are indicated as follows: Queensland-Australia (QLD); Papua-New Guinea (PNG); Solomon Islands (SI); Vanuatu Islands (VA); New Caledonia (NC). The cruise track is represented by the blue line.

## 2.1. Principle

[8] The velocity field between each station pair is calculated, relative to 2000 m, from temperature and salinity through geostrophic balance. At the surface, the wind-driven water transport is determined by the Ekman relation from the August 2007 blended monthly average winds of the NOMADS (<http://nomads.nccdc.noaa.gov>). Using the Gauss-Markov least-square estimate, velocities at 2000 m (and thereby to the whole water column) are adjusted to accommodate conservation constraints within isopycnal layers bounded by the sections forming the box, as described in *Ganachaud and Wunsch [2000]*.

## 2.2. Additional Constraints

[9] In addition to mass and property conservation, the total transport between New Caledonia and PNG, the air-sea fluxes, and the a priori velocity field, were also constrained. The total transport between New Caledonia and PNG was estimated, independently, at  $10 \pm 5$  Sv westward based on two ocean products (August 2007 average from the BlueLink Reanalysis [*Schiller et al., 2008*] and from the Mercator Ocean PSY3 [*Larnicol et al., 2006*]; with uncertainty from 1 std of daily values). We also accounted for a westward transport of  $4 \pm 3$  Sv through the *Grand Passage* ( $18^\circ 30' \text{S}$ ) between the main reef of New Caledonia and its northern atoll [*Gasparin et al., 2011*]. The surface heat flux inside the closed area was constrained at  $50 \pm 50 \text{ W} \cdot \text{m}^{-2}$  to the atmosphere, based on NCEP products.

[10] Velocity profiles from the L-ADCP attached to the measurement rosette provided an independent constraint on the velocity field. Including S-ADCP data in the process

[*Visbeck, 2002*], those were projected along the direction of geostrophic velocities, averaged between station pairs and compared with the geostrophic velocity profile (Figure S2 in the auxiliary material).<sup>1</sup> Most profiles were in agreement (rms difference  $< 4 \text{ cm} \cdot \text{s}^{-1}$  between 1000 m and 2000 m), which permitted to constrain a priori velocities and uncertainties at the reference level, with the 1000 m–2000 m depth-averaged L-ADCP [*Casal et al., 2009*; *Gasparin et al., 2011*]. The corresponding a priori uncertainties were set at  $\pm 2 \text{ cm} \cdot \text{s}^{-1}$ , except just north of New Caledonia where diverging L-ADCP/geostrophy shears led to a larger a priori uncertainty  $\pm 10 \text{ cm} \cdot \text{s}^{-1}$ .

[11] For our mass transport estimates, we also accounted for an 8-Sv “leak” between station 15 and PNG (Figure 1). The transport through this leak was estimated by extrapolation of L-ADCP currents between station 15 and the coast. While the leak is not directly part of the inversion, it is included in the total Gulf of Papua Current (GPC) and NGCU (New Guinea Coastal Undercurrent) transport estimates (values in parentheses in Figure 1).

## 3. Results

### 3.1. Main Currents and Integral Transports

[12] From this inverse model, the total northbound flow into the Solomon Sea is estimated at  $29 \pm 5$  Sv (hereafter, and unless otherwise specified, we refer to transports above 1300 m, which corresponds to the depth of northward or

<sup>1</sup>Auxiliary materials are available in the HTML. doi:10.1029/2012GL052575.

eastward flow reached by the major currents). This includes the  $8 \pm 2$  Sv estimated “leak” between the PNG reefs and the closest hydrographic profile (Figure 1; section 2). Accounting for this leak, the western boundary current is estimated at  $29 \pm 3$  Sv ( $26 \pm 4$  above 2000 m) eastward south of Sudest/Rossel islands where it is now called the *Gulf of Papua Current* [SPICE Community, 2012]. From a 1993 survey of the World Ocean Circulation Experiment, this transport was estimated at a similar value of 26 Sv by Sokolov and Rintoul [2000]. Through the central section, we find that the full GPC transport outflows into the Solomon Sea, where it becomes the NGCU (Figure 1), with a transport of  $29 \pm 3$  Sv ( $30 \pm 4$  Sv above 2000 m) including the leak. This circulation implies a sharp anticlockwise turn ( $>90^\circ$ ) to the north around the tip of Rossel Island, within 160 km of the coast, a feature also observed in direct current observations of the thermocline currents [Cravatte et al., 2011]. Centered on  $157^\circ$ S, another  $7 \pm 3$  Sv contribute to the supply into the Solomon Sea, which is part of the “direct” inflow from the Coral Sea [Qu and Lindstrom, 2002], as discussed below. On the east side of the Solomon Sea,  $10 \pm 2$  Sv are feeding back into the Coral Sea. This southward flow was not observed so far, and numerical simulations [Melet et al., 2010] suggest that it originates in the east part of the Solomon Strait, therefore carrying equatorial waters to the South (see below). To the east, in front of Indispensable Strait, a strong southwestward flow carries  $8 \pm 2$  Sv, which necessarily comes from the east of the Solomon Islands, and partially turns northwestward against Guadalcanal to feed the Solomon Sea, and eastward south of Makira. A flow through this strait was suspected [Andrews and Clegg, 1989; Melet et al., 2010], but never measured yet. Finally, the flow south of Makira is dominated by the westward North Vanuatu Jet (NVJ,  $22 \pm 3$  Sv), which is an essential supply of the Coral Sea [Gourdeau et al., 2008].

### 3.2. Vertical Structure and Water Properties

[13] Measured ocean salinity and dissolved oxygen content guided our analysis of water mass origins and circulation patterns. Above 2000 m, the main water masses are identified by two prominent features: a strong maximum in salinity near 150 m depth characterizes the South Pacific Tropical Water (SPTW) which originates in the central South Pacific [Donguy, 1994] ( $\sigma = 24.5$ ; see Figure S1). Near 500–600 m, the core layer of the Antarctic Intermediate Waters (AAIW) emanating from southern higher latitudes, is characterized by a salinity minimum and an oxygen maximum [Qu and Lindstrom, 2002] ( $\sigma = 27.1$ ; see Figure S1). In the following, we relate the main currents to horizontal structures within these layers of extrema.

[14] The vertical structure reveals strong currents, concentrated above 1300 m, with velocities sometimes larger than  $50 \text{ cm.s}^{-1}$  (Figure 2a). The independent direct velocity measurements from a L-ADCP, compared quantitatively with geostrophic currents referenced at 2000 m (Figure S2), attested the accuracy of the geostrophic approach. L-ADCP data were then used as a reference to the velocity at depths (see Section 2), which confirmed the general structure of the currents and revealed undocumented countercurrents below 1300 m. Boundary integrals for transports estimation were defined from both water mass properties and estimated cumulative transports (Figure 2c). South of Sudest Island (WEST section, Figure 2a, left), the GPC reaches velocities

of  $\sim 50 \text{ cm.s}^{-1}$ , with a deep core close to 400 m depth. The geostrophic velocities disagree with L-ADCP data (Figure S2) between station 10 and 13 which we attribute to the confluence of an internal wave at station 12, with no incidence on mass and property budgets [Ganachaud, 2003]. The GPC core is marked by highest oxygen content at intermediate levels (core A, 500 m, Figure 2b), originating from the Coral Sea western boundary currents as suggested by water properties [Sokolov and Rintoul, 2000; Qu and Lindstrom, 2002] (Figure S3). Below the GPC core, a countercurrent carries  $3 \pm 2$  Sv of low oxygen waters to the west (core B, Figure 2b).

[15] In the CENTRAL section (Figure 2a, middle), the main core of the western boundary current, the NGCU, occupies the upper  $\sim 1300$  m, with again the strongest oxygen content at intermediate levels (core C, Figure 2b) overlying a southward countercurrent of low oxygen content (core D, Figure 2b). To the east of the NGCU, the flow is mostly northward at thermocline level, in the “DIRECT” pathway ( $156\text{--}157^\circ$ E). Below that, there is no net flow of intermediate waters, recirculations at moderate oxygen content (zone E-E, Figures 2b and 2c). The southward flow centered on  $158.5^\circ$ E (North Solomon waters, N.SOL) is found to be prominent in the thermocline waters (Figures 2a and 2c), with a marked low oxygen (zone F-F, Figure 2b), and relatively lower salinity (not shown). These properties indicate an origin in the SEC waters from the east of the Solomon Islands, that entered the Solomon Strait after flowing along the east margin of the Solomon Islands [Qu and Lindstrom, 2002] (Figure S3). Those waters would then flow southeastward in the eastern part of the Solomon Sea [Melet et al., 2010; Hristova and Kessler, 2012]. Conversely, at intermediate levels, the flow below the southward N.SOL is weaker, and partially northward, suggesting differing pathways for intermediate and thermocline waters in this area.

[16] The flow through Indispensable section (INDIS) is southwestward in the northern part of the section, marked by an anomalous low oxygen content in both thermocline and intermediate waters (cores G-G, Figure 2b), indicating an origin from the eastern side of Indispensable Strait (Figure S3). These low oxygen waters are also found south of both Guadalcanal and Makira islands, in relation with northwestward and eastward coastal currents, respectively. Across the EAST section (Figure 2, left), flow is mostly westward, with the NVJ core above 400 m near  $13^\circ$ S, a relatively shallow depth, as noted earlier [Gourdeau et al., 2008].

## 4. Discussion

[17] A general circulation scheme appears from the transport estimate, and water properties reported against transports reveals the connection between the currents. For conciseness, we only present dissolved oxygen, but salinity patterns confirm our conclusions (Figure S4). At thermocline level, highest dissolved oxygen levels are found at the northern tip of New Caledonia ( $\sim 18^\circ$ S). Those high values appear again in the GPC and NGCU currents, near Sudest and Rossel islands (Figure 3a), but at lower concentrations as expected from biological remineralization. These regions of high oxygen are confirmed by climatology [Ridgway and Dunn, 2003] (e.g., Figure S3), and consistent with a connection through the GPC pathway in the Coral Sea

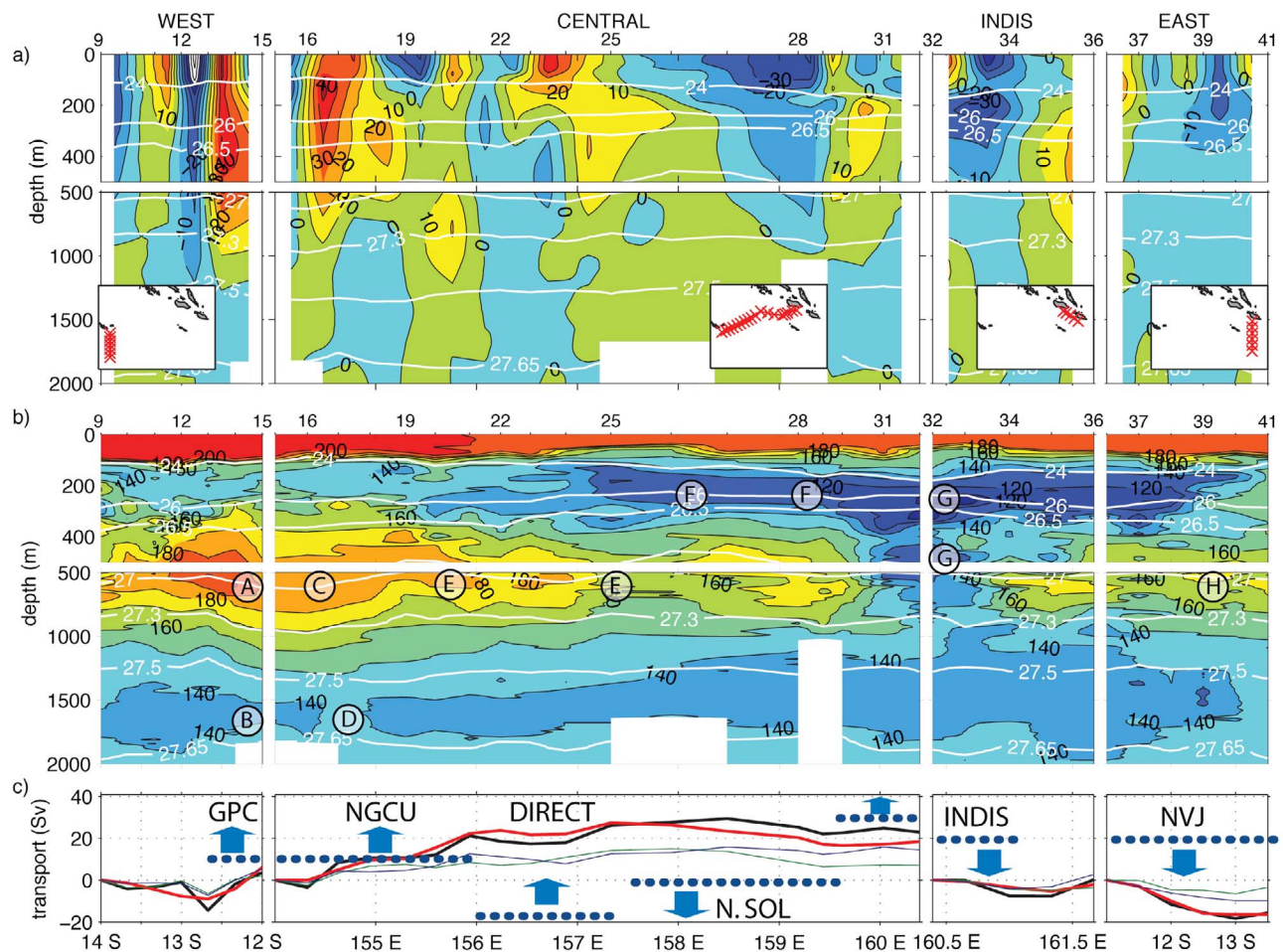


**Figure 2.** Estimated oceanic currents and measured dissolved oxygen concentration. (a) Geostrophic currents (in  $\text{m}\cdot\text{s}^{-1}$ ), perpendicular to the sections, referenced to 2000 m and adjusted through the inverse box model. Positive is either eastward or northward; key isopycnal layers are provided (white contours). The panel displays 4 sections called WEST, CENTRAL, INDIS and EAST, with station positions indicated in the inset of each panel and station number above the panels. (b) Same as Figure 2a but for dissolved oxygen concentration (in  $\mu\text{mol}\cdot\text{l}^{-1}$ ). Key property cores are indicated by the encircled letters, referred to in the text. (c) Estimated water mass transports (black line), cumulative from the left end of each section, integrated from the surface to 2000 m depth, with the name of the currents referred to in the text. Layer transports are indicated by the thin lines: surface to  $\sigma = 26.5$  (green) and  $\sigma = 26.5\text{--}27.5$  (blue). The red line indicates transports from L-ADCP-only data. The blue arrows indicate the direction of the current; the dark blue dots indicate the width of each current. Latitude/longitude are indicated at the bottom of the figure, according to the orientation of the section.

(inset of Figure 1) [Sokolov and Rintoul, 2000; Qu and Lindstrom, 2002]. It also confirms the tight continuity between the GPC south of Sudest Island, on the WEST section and the NGCU east of Rossel Island. Thermocline oxygen concentrations of the DIRECT inflow ( $\sim 155^\circ\text{E}$ ,  $\sim 12^\circ\text{S}$ ) are much lower than those of the NGCU, but consistent with the lowest oxygen from NVJ and N.SOL inflows. This, along with salinity contents (Figure S4), indicates contributions from the Coral Sea to this DIRECT inflow into the Solomon Sea. Southeast of Guadalcanal (Figure 3a,  $159^\circ\text{E}$ ), the low oxygen/moderate salinity waters necessarily emanates from a mixture of Indispensable Strait and N.SOL (Figure S3). At intermediate level (Figure 3b), remarks similar to those for thermocline levels hold concerning the GPC/NGCU pathway. There is no coherent DIRECT nor N.SOL transports (Figure 2c). But waters from the Indispensable Strait are distinct, with lower oxygen content whose signature is traced

back in the outflows east of Guadalcanal and south of Makira (arrows on Figure 3b). At deeper levels (Figure 3c), the circulation mostly reverses, with water properties indicating a supply of the GPC countercurrent by the NGCU countercurrent. To the east, waters from the north of the Solomon Sea flows southward near the Solomon Islands and northeastward through the Indispensable Strait, again with similar properties. This deep circulation pattern was not documented so far, and repeated observations are needed to confirm its persistence.

[18] The warm currents we described transport large amounts of internal (heat) energy and their pathways can condition the patterns of sea surface temperature and heat release to the atmosphere. Referring to the integral 0–2000 m transport for a temperature on the  $^\circ\text{C}$  scale, the GPC and NGCU transport  $1.4 \pm 0.2$  PW (1 PW =  $10^{15}$  W), for a total inflow of  $1.0 \pm 0.3$  PW through the CENTRAL section into

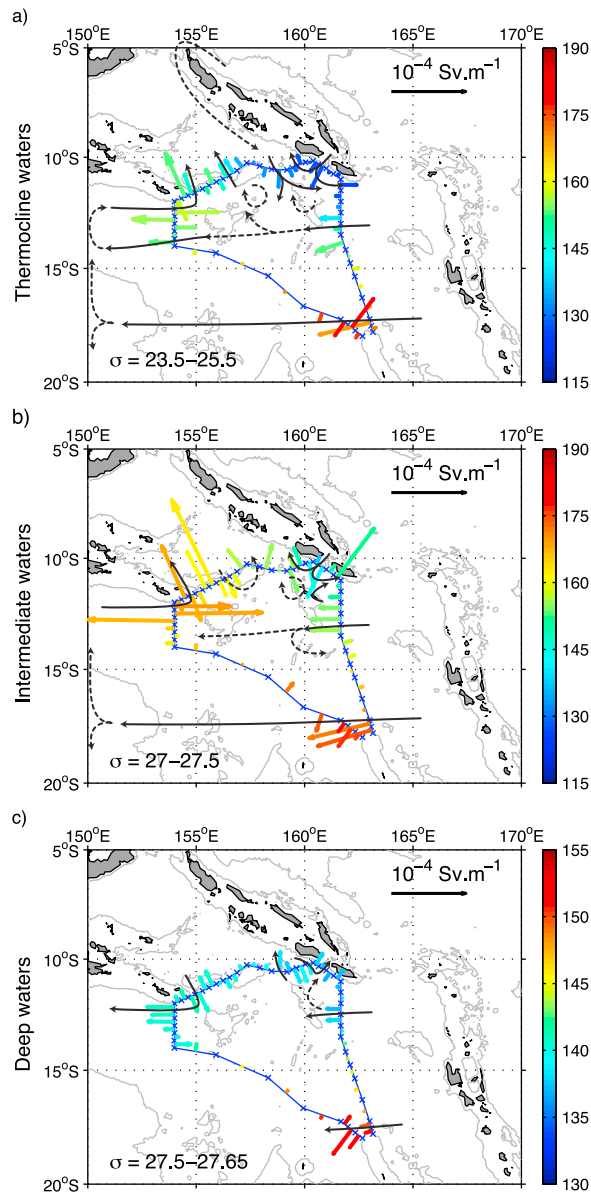


**Figure 3.** Transport against dissolved oxygen concentration for selected layers (in  $\mu\text{mol.l}^{-1}$ ). (a) Thermocline layer, defined between densities  $\sigma = 23.5 - \sigma = 25.5$ . (b) Intermediate layer ( $\sigma = 27.0 - \sigma = 27.5$ ) and (c) deep layer ( $\sigma = 27.5 - \sigma = 27.65$ ). Transport is normalized horizontally ( $\text{Sv.m}^{-1}$ , scale in the upper right of the panels); the arrow color gives the averaged dissolved oxygen. The solid black arrows correspond to the pathways deduced from both calculated transports and water properties; the dashed arrows correspond to pathways or mixing (circular arrow) deduced from water mass properties.

the Solomon Sea, including the Ekman surface transport for the later ( $-0.25$  PW). The Indispensable Strait brings  $0.25 \pm 0.1$  PW into the Solomon Sea, so that the contribution from the Coral Sea is of  $0.75 \pm 0.3$  PW. This corresponds to 50% of the SEC inflow of energy into the Coral Sea, between Makira and New Caledonia ( $1.6 \pm 0.2$  PW). For comparison, the internal energy transported between the

Pacific and Indian was estimated at 1.4 PW by Ganachaud and Wunsch [2000].

## 5. Conclusion

[19] From a high-resolution hydrographic survey, we estimate the net mass and internal energy transports entering the Solomon Sea above 1300 m respectively at  $29 \pm 5$  Sv ( $1 \text{ Sv} = 10^6 \text{ m}^3 \cdot \text{s}^{-1}$ ) and  $1.0 \pm 0.3 \cdot 10^{15}$  W, and describe the extremely sharp bend of the western boundary current around the south-east tip of Papua New Guinea.

[20] Through these massive transports, climate signals and water properties can be transmitted efficiently from the South Pacific gyre to the equator. These new results support the strong role of the southwest Pacific oceanic circulation in the equatorial system which is one of the main hypothesis at the basis of the SPICE project.

[21] But in a region of complicated topography, realistic numerical simulations are difficult to achieve, in particular in IPCC-class ocean models [Sen Gupta et al., 2012], and these new results will provide a benchmark, not only to mass and internal energy transports, but also to micro nutrients which are the main fertilizers of the equatorial ecosystem [Grenier et al., 2011]. Nevertheless, repeated measurements such as those from ocean gliders will be essential to refine estimates in this region of high variability [Davis et al., 2012].

[22] **Acknowledgments.** This work is co-funded by ANR (ANR-09-BLAN-0233-01); INSU/LEFE/IDAO (Solwara), and the French Ministry for Education and Research (MESR); it is a contribution to the CLIVAR/SPICE International programme. The FLUSEC cruise was supported by IRD and LEGOS. We are particularly grateful to the R/V Alis crew and the IRD staff, as well as to both governments of PNG and the Solomon Islands. The contributions by D. Varillon, J. Lefèvre, J. Sudre, L. Goudeau and A. Melet were essential to the data set. This work benefitted from essential input by S. Cravatte.

[23] The Editor thanks two anonymous reviewers for assisting in the evaluation of this paper.

## References

- Andrews, J. C., and S. Clegg (1989), Coral Sea circulation and transport deduced from modal information models, *Deep Sea Res., Part A*, 36(6), 957–974, doi:10.1016/0198-0149(89)90037-X.
- Casal, T. G. D., L. M. Beal, R. Lumpkin, and W. E. Johns (2009), Structure and downstream evolution of the Agulhas Current system during a quasi-synoptic survey in February–March 2003, *J. Geophys. Res.*, 114, C03001, doi:10.1029/2008JC004954.
- Cravatte, S., A. Ganachaud, Q. Duong, W. S. Kessler, G. Eldin, and P. Dutrioux (2011), Observed circulation in the Solomon Sea from SADCP data, *Prog. Oceanogr.*, 88(1–4), 116–130, doi:10.1016/j.pocan.2010.12.015.
- Davis, R., W. S. Kessler, and J. Sherman (2012), Gliders measure western boundary current transport from the South Pacific to the equator, *J. Phys. Oceanogr.*, in press.
- Donguy, J. R. (1994), Surface and subsurface salinity in the tropical Pacific Ocean relations with climate, *Prog. Oceanogr.*, 34(1), 45–78, doi:10.1016/0079-6611(94)90026-4.
- Ganachaud, A. (2003), Error budget of inverse box models: The North Atlantic, *J. Atmos. Oceanic Technol.*, 20(11), 1641–1655.
- Ganachaud, A., and C. Wunsch (2000), Improved estimates of global ocean circulation, heat transport and mixing from hydrographic data, *Nature*, 408(6811), 453–457, doi:10.1038/35044048.
- Ganachaud, A., et al. (2007), Southwest Pacific Ocean Circulation and Climate Experiment (SPICE). Part 1. Scientific background, technical report, NOAA, Silver Spring, Md.
- Gasparin, F., A. Ganachaud, and C. Maes (2011), A western boundary current east of New Caledonia: Observed characteristics, *Deep Sea Res., Part I*, 58, 956–969.
- Gourdeau, L., W. S. Kessler, R. E. Davis, J. Sherman, C. Maes, and E. Kestenare (2008), Zonal jets entering the Coral Sea, *J. Phys. Oceanogr.*, 38(3), 715–725.
- Grenier, M., S. Cravatte, B. Blanke, C. Menkes, A. Koch-Larrouy, F. Durand, A. Melet, and C. Jeandel (2011), From the western boundary currents to the

- Pacific Equatorial Undercurrent: Modeled pathways and water mass evolutions, *J. Geophys. Res.*, *116*, C12044, doi:10.1029/2011JC007477.
- Gu, D., and S. G. Philander (1997), Interdecadal climate fluctuations that depend on exchanges between the tropics and extratropics, *Science*, *275*, 805–807, doi:10.1126/science.275.5301.805.
- Hristova, H. G., and W. S. Kessler (2012), Surface circulation in the Solomon Sea derived from Lagrangian drifter observations, *J. Phys. Oceanogr.*, *42*, 448–458, doi:10.1175/JPO-D-11-099.1.
- Larnicol, G., S. Guinehut, M. H. Rio, M. Drevillon, Y. Faugere, G. Nicolas (2006), The global observed ocean products of the french Mercator project, in *Proceedings of 15 Years of Progress in Radar Altimetry Symposium*, *Eur. Space Agency Spec. Publ.*, ESA SP-614.
- Lindstrom, E., R. Lukas, R. A. Fine, J. S. Godfrey, G. Meyers, and M. Tsuchiya (1987), The western equatorial Pacific ocean circulation study, *Nature*, *330*, 533–537.
- Maes, C., G. Eldin, A. Melet, J. Lefèvre, J. Sudre, D. Varillon, A. Ganachaud, and L. Gourdeau (2008), FLUSEC-01 cruise report, 12–30 August 2007, *Rep. 24*, Cent. IRD de Nouméa, Nouméa, New Caledonia.
- Melet, A., L. Gourdeau, W. S. Kessler, J. Verron, and J. Molines (2010), Thermocline circulation in the Solomon Sea: A modeling study, *J. Phys. Oceanogr.*, *40*(6), 1302–1319, doi:10.1175/2009JPO4264.1.
- Qu, T., and E. J. Lindstrom (2002), A climatological interpretation of the circulation in the western South Pacific, *J. Phys. Oceanogr.*, *32*(9), 2492–2508.
- Ridgway, K., and J. R. Dunn (2003), Mesoscale structure of the mean East Australian Current system and its relationship with topography, *Prog. Oceanogr.*, *56*(2), 189–222, doi:10.1016/S0079-6611(03)00004-1.
- Schiller, A., P. R. Oke, G. Brassington, M. Entel, R. Fiedler, D. A. Griffin, and J. V. Mansbridge (2008), Eddy-resolving ocean circulation in the Asian–Australian region inferred from an ocean reanalysis effort, *Prog. Oceanogr.*, *76*, 334–365.
- Sen Gupta, A., A. Ganachaud, S. McGregor, J. N. Brown, and L. Muir (2012), Drivers of the projected changes to the Pacific Ocean equatorial circulation, *Geophys. Res. Lett.*, *39*, L09605, doi:10.1029/2012GL051447.
- Sokolov, S., and S. Rintoul (2000), Circulation and water masses of the Southwest Pacific: WOCE section p11, Papua New Guinea to Tasmania, *J. Mar. Res.*, *58*(2), 223–268.
- SPICE Community (2012), Naming a western boundary current from Australia to the Solomon Sea, *CLIVAR Newsl. Exchanges*, *16*(56), 28.
- Visbeck, M. (2002), Deep velocity profiling using acoustic Doppler current profilers: Bottom tracks and inverse solutions, *J. Atmos. Oceanic Technol.*, *19*, 794–807.
- Wyrtki, K. (1975), El Niño—The dynamic response of the equatorial Pacific Ocean to atmospheric forcing, *J. Phys. Oceanogr.*, *5*, 572–584, 19, 794–807.